Soft Matter

Accepted Manuscript

ROYAL SOCIETY OF CHEMISTRY

www.rsc.org/softmatter

Soft Matter

Dynamic Article Links ►

Cite this: DOI: 10.1039/c0xx00000x

www.rsc.org/xxxxxx

ARTICLE TYPE

Toward Dynamic Phase Transition Mechanism of a Thermoresponsive Ionic Liquid in the Presence of Different Thermoresponsive Polymers

Ge Wang and Peiyi Wu*

Received (in XXX, XXX) Xth XXXXXXXXX 20XX, Accepted Xth XXXXXXXXX 20XX

DOI: 10.1039/b000000x

The influence of two thermoresponsive polymers, poly(N-isopropylacrylamide) (PNIPAM) and poly(N-vinylcaprolactam) (PVCL), on the phase transition behavior of a thermoresponsive ionic liquid, tributylhexylphosphonium 3-sulfopropylmethacrylate ([$P_{4,4,4,6}$][MC3S]), was investigated. Obvious distinction was observed in the LCSTs and morphologies between [$P_{4,4,4,6}$][MC3S]-PNIPAM and [$P_{4,4,4,6}$][MC3S]-PVCL aqueous solutions, indicating their large differences in dynamic transition processes. In general, PNIPAM can "break" the water structure of [$P_{4,4,4,6}$][MC3S] to decrease the transition temperature, while PVCL can "make" the water structure to increase it. Surprisingly, [$P_{4,4,4,6}$][MC3S] has an unusual over-hydration behavior before dehydration while PNIPAM experiences a two-step transition process in [$P_{4,4,4,6}$][MC3S]-PNIPAM aqueous solution, which has never been reported so far. Further studies revealed that the formation of strong intra-/inter-molecular hydrogen bond C=O···D–N in PNIPAM is the driving force for the LCST phenomenon of [$P_{4,4,4,6}$][MC3S]-PNIPAM solution, while it is the [$P_{4,4,4,6}$][MC3S] that dominates the phase separation of [$P_{4,4,4,6}$][MC3S]-PVCL solution.

Introduction

Ionic liquids (ILs) are organic salts whose melting points are very low (below 100 °C or even at room temperature).[1, 2] They have many unique properties (excellent ionic conductivities, broad electro-chemical window, high thermal and chemical stability and negligible vapor pressure, *etc.*), which can be flexibly tuned by combining different cations and anions. According to estimation, more than a million potential cation/anion-combinations are available and provide unlimited possibility for ILs to be applied in many specific areas.[3] Hence, the research into ILs is booming. ILs have been widely investigated in various fields including organic synthesis[4-6], catalysis[6-8], electrochemistry[9,10], analytical chemistry[11, 12], separation[13, 14] and polymer chemistry[15-18].

As a typical example of charged organics, ILs have multiple interactions with many substances including solvents[19], celluloses[20], proteins[21] and polymers especially thermoresponsive polymers[22-24]. Among a great variety of thermoresponsive polymers, poly(*N*-isopropylacrylamide) (PNIPAM) with a lower critical solution temperature (LCST ~32 °C) close to physiological temperature has been widely studied. In 2011, Venkatesu investigated the effect of an imidazolium-based IL, 1-benzyl-3-methylimidazolium tetrafluoroborat ([Bzmim][BF_4]), on the LCST behavior of PNIPAM in aqueous solution.[22] Their experimental results elucidated that [Bzmim][BF_4] destabilizes the hydrated macromolecule structure and reduces the LCST of PNIPAM. Our group observed that 1-butyl-3-methylimidazolium tetrafluoroborate ([Bmim][BF_4]) acts as the "destroyer" and the "constructer" for the phase behavior of PNIPAM.[23] Besides PNIPAM, poly(*N*-vinylcaprolactam) (PVCL) is another well-studied thermoresponsive polymer. Lately, we investigated the thermodynamic phase behavior of PVCL solution in the presence of different hydrophilic/hydrophobic ILs.[24] The addition of hydrophilic ILs hardly affects the transition temperature of PVCL, while the addition of hydrophobic ILs, such as 1-ethyl-3-methylimidazolium bis(trifluoromethylsulfonyl) imide ([Emin][NTf_2]), can increase it. In general, related studies are rare and have focused on ternary composite systems, in which the interactions are versatile and complex. However, only conventional ILs are involved in these systems and ILs are used merely as additives.

Recently, thermoresponsive ionic liquids, especially LCST-type ILs, have been attracting much interest in ILs science. As a distinct subclass of ILs, LCST-type ILs exhibit unique advantages in many applications.[25-27] More and more studies have focused on the phase separation behavior of ILs, or even poly(ionic liquid)s (PILs). In 2007, the LCST-type phase transition of amino-acids-based ILs was reported by Ohno's group.[28] To the best of our knowledge, this system is the first example for LCST-type behavior of IL/water mixtures. By adjusting the balance of hydrophilicity and hydrophobicity, a series of LCST-type ILs have been synthesized.[29, 30] In 2012, Ohno's group first reported the LCST-type phase transition behavior of PILs in pure water.[31, 32] More recently, a series of new

---

State Key Laboratory of Molecular Engineering of Polymers, Collaborative Innovation Center of Polymers and Polymer Composite Materials, Department of Macromolecular Science and Laboratory for Advanced Materials, Fudan University, Shanghai 200433, China
E-mail: peiyiwu@fudan.edu.cn

LCST-type ILs (TVBP-CxS) and its polymers, cationic PILs, were reported by Yuan's group.[33] Nevertheless, the study of thermoresponsive ILs is still in its infancy, and current research works are confined to binary systems that only involve the thermoresponsive ILs and solvents (water in most cases). Moreover, there is no example of studying the interactions between thermoresponsive ILs and thermoresponsive polymers so far, let alone the integrated mechanism of the phase transition on the molecular level. Studying the interactions between thermoresponsive ILs and thermoresponsive polymers is helpful for comparing the difference of them, as well as further understanding the transition behavior of ILs. In consideration of the unique properties of ILs and thermoresponsive polymers, the combination of thermoresponsive polymers with LCST-type ILs could not only broaden their own applications, but also be proposed for the application in new field. Under this circumstance, comprehension of the interactions between LCST-type ILs and thermoresponsive polymers becomes very essential and attractive to study.

In the present work, we designed a ternary composite system composed of a LCST-type IL, tributylhexylphosphonium 3-sulfopropylmethacrylate ([$P_{4,4,4,6}$][MC3S]), thermoresponsive polymers and water to explore the effect of thermoresponsive polymers on the LCST behavior of IL and the interactions between IL and the polymers at the same time. Moreover, the phase separation mechanism of [$P_{4,4,4,6}$][MC3S] has been clarified recently[34], which provides convenience for studying thermoresponsive IL-included ternary complex systems. As for thermoresponsive polymers, we chose PNIPAM and PVCL as two typical examples. PNIPAM is the most familiar LCST-type polymer whose phase separation undergoes a coil–globule transition.[35] As a type I thermoresponsive polymer, PVCL shows a continuous phase transition behavior with liquid–liquid phase separation (LLPS).[36, 37] The influence of different thermoresponsive polymers on the LCST-type phase transition of [$P_{4,4,4,6}$][MC3S] solution was first elucidated by DSC, optical microscopy, NMR, FT-IR in combination with perturbation correlation moving window (PCMW) technique, which is very helpful to further understand the interactions of other thermoresponsive ILs involved systems.

Experimental

Materials

N-isopropylacylamide (NIPAM) was purchased from Aladdin Reagent Co. and recrystallized from cyclohexane prior to polymerize. *N*-vinylcaprolactam (VCL) was obtained from Alfa Aesar Co. and purified by passing through a short alumina column prior to use. 2,2'-Azobis(2-isobutyronitrile) (AIBN; Aladdin Reagent Co.) was recrystallized from ethanol. Tributylhexylphosphonium bromide ([$P_{4,4,4,6}$][Br]; Beijing HWRK Chem Co.), potassium 3-sulfopropylmethacrylate ([K][MC3S]; Aladdin Reagent Co.) and deuterium oxide (D_2O, D-99.9%; Cambridge Isotope Laboratories Inc.) were used as received.

Sample preparation

The detailed synthesis procedures are shown in the ESI†.

Differential scanning calorimetry (DSC)

Calorimetric measurements were performed on the Mettler–Toledo differential scanning calorimetry (DSC) thermal analyzer with a scanning rate of 10 ^{o}C/min. Additionally, the testing temperature of the DSC ranged from 10 to 70 ^{o}C.

Optical microscopy

Optical microscopy observations were carried out on Leica DM2500P polarizing microscope with a Linkam THMS600 hot stage to control the experimental temperature, whose sensor accuracy is 0.1 ^{o}C. The heating rate is 0.5 ^{o}C/min for [$P_{4,4,4,6}$][MC3S]-PNIPAM and [$P_{4,4,4,6}$][MC3S]-PVCL aqueous solutions.

Temperature-variable ^{1}H nuclear magnetic resonance (^{1}H NMR)

Temperature-variable ^{1}H NMR spectra of [$P_{4,4,4,6}$][MC3S] D_2O solution (20% (w/v)) and 20% (w/v) [$P_{4,4,4,6}$][MC3S]-D_2O with 4% (w/v) PNIPAM or PVCL (polymers/IL = 20 wt%) were recorded on Varian Mercury plus (400 MHz) spectrometer at a rate of 0.5 ^{o}C/min. For [$P_{4,4,4,6}$][MC3S]-PNIPAM-D_2O solution, the testing temperature ranged from 15 to 40 ^{o}C; while for [$P_{4,4,4,6}$][MC3S]-D_2O and [$P_{4,4,4,6}$][MC3S]-PVCL-D_2O solutions, the heating range was 25 to 50 ^{o}C. All the spectra were obtained using the same instrumental parameters.

Fourier transform infrared spectroscopy (FT-IR)

The solutions of 20% (w/v) [$P_{4,4,4,6}$][MC3S]-D_2O with 4% (w/v) PNIPAM and 20% (w/v) [$P_{4,4,4,6}$][MC3S]-D_2O with 4% (w/v) PVCL were sealed between two ZnS tablets for FT-IR measurements. All temperature-dependent FT-IR spectra were collected on a Nicolet Nexus 6700 spectrometer with a DTGS detector. 32 scans at a resolution of 2 cm^{-1} were accumulated to achieve acceptable high-quality spectra. Temperatures were controlled with electronic cell holder at a rate of 0.5 ^{o}C/min with an increment of 1 ^{o}C (accuracy is 0.1 ^{o}C). After all spectra were collected, the original spectra were baseline-corrected by the software Omnic 6.1a. Collected from 15 to 40 ^{o}C for [$P_{4,4,4,6}$][MC3S]-PNIPAM and 25 to 50 ^{o}C for [$P_{4,4,4,6}$][MC3S]-PVCL, the FT-IR spectra were used for conventional analysis and further two-dimensional analysis.

Perturbation correlation moving window (PCMW)

The temperature-dependent FT-IR spectra for different chemical groups in certain wavenumber ranges were selected to carry out PCMW analysis. The method provided by Morita was utilized to process raw data. The further correlation information was calculated by the software 2D Shige, *ver.* 1.3 (©Shigeaki Morita, Kwansei Gakuin University, Japan, 2004–2005) with an appropriate window size ($2m + 1 = 11$) to generate quality PCMW spectra. Finally, the contour maps were plotted by Origin Program *ver.* 8.0 with warm colors (red and yellow) indicating positive intensities while cool colors (blue) indicating negative ones.

Results and discussion

Calorimetric measurements

To elucidate the effect of different thermoresponsive polymers on the phase transition behavior of [P$_{4,4,4,6}$][MC3S] solution, differential scanning calorimetric measurements were performed. Figure 1 presents the heating curves of [P$_{4,4,4,6}$][MC3S] solutions with different weight ratios of PNIPAM (a) and PVCL (b). The phase separation of pure IL solution (20% (w/v)) occurs at 37 ^{o}C with a broad and asymmetric endothermic peak. For lacking of strong self-associated hydrogen bonds, [P$_{4,4,4,6}$][MC3S] experiences a gradual change above LCST similar to PVCL[36] and poly(oligo(ethylene glycol) methacrylate) (POEGMA)[38], but different from PNIPAM[39].

Surprisingly, when 4% (w/v) PNIPAM (PNIPAM/IL = 20 wt%) has been added, the LCST of the mixed solution decreases drastically to 25 ^{o}C, which is lower than pure IL solution (*ca.* 37 ^{o}C) and pure PNIPAM solution (*ca.* 32 ^{o}C, in Figure S2 (a)). With the weight ratio of PNIPAM to IL increasing from 20 to 100 wt%, the transition temperatures of the PNIPAM-involved IL solutions maintain at 25 ^{o}C. The endothermic peaks tend to increase and become narrow and symmetric, whose shape approach those of pure PNIPAM solutions (seen in Figure S2 (a)). As the result, we surmise that PNIPAM dominates the phase separation of PNIPAM-involved IL solutions, even if the weight ratio of PNIPAM is low. The case is totally different for the PVCL-involved system, the LCST of IL solution mixed with 4% (w/v) PVCL (PVCL/IL = 20 wt%) is 39 ^{o}C, which is the middle of pure IL solution (*ca.* 37 ^{o}C) and pure PVCL solution (*ca.* 41 ^{o}C, in Figure S2 (b)). However, the distinction is small in comparison to the PNIPAM-involved system. What's more, the transition temperatures of the PVCL-involved IL solutions rise gradually as the weight ratio of PVCL to IL increases from 20 to 100 wt%, which is similar to the tendency of pure PVCL solutions (seen in Figure S2 (b)). Different from PNIPAM-involved system, the endothermic peaks of PVCL-involved IL solutions are broad and asymmetric and the sizes are almost unchanged. This phenomenon reveals that the phase separation of PVCL-involved IL solution is a gradual dehydration process and the large amounts of IL dominant the LCST behavior of PVCL-involved IL solutions.

Generally, the addition of PNIPAM into [P$_{4,4,4,6}$][MC3S] solution can drastically decrease the LCST of [P$_{4,4,4,6}$][MC3S], while the addition of PVCL increases it. It is well-known that the combination of salts with polymer or protein would affect the behavior of salts and polymer or protein through their interactions with water.[40, 41] The thermoresponsive polymers added into the [P$_{4,4,4,6}$][MC3S] solution can interact with water and induce changes in the interaction between IL and water. This indirect effect of the polymers may alter the transition temperatures of LCST-type IL solutions. Specifically, PNIPAM can "break" the water structure to decrease the transition temperature of [P$_{4,4,4,6}$][MC3S] solution, while PVCL can "make" the water structure to increase it. Moreover, the phase diagrams in Figure S3 and Figure S4 illustrate the LCST variation of IL-included ternary systems and pure thermoresponsive polymers solutions with different concentrations, respectively. To further study the distinction between PNIPAM and PVCL on the phase transition behavior of [P$_{4,4,4,6}$][MC3S], we chose 20% (w/v) [P$_{4,4,4,6}$][MC3S] with 4% (w/v) PNIPAM or PVCL (polymers/IL = 20 wt%) for the following experiments.

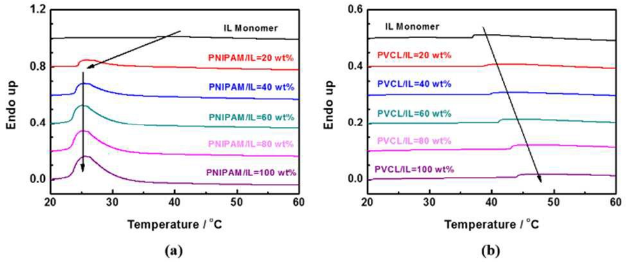

Figure 1. DSC heating curves of 20% (w/v) [P$_{4,4,4,6}$][MC3S] with addition of (a) PNIPAM and (b) PVCL whose weight ratios are 0, 20, 40, 60, 80, 100 wt% to [P$_{4,4,4,6}$][MC3S] at a scanning rate of 10 ^{o}C/min.

Optical microscopy

Optical microscopy was performed to directly observe the temperature-induced phase transition of IL-included ternary systems. The optical microscopy photographs of [P$_{4,4,4,6}$][MC3S]-PNIPAM (15-40 ^{o}C) and [P$_{4,4,4,6}$][MC3S]-PVCL (25-50 ^{o}C) solutions are shown in Figure 2. When the temperature reaches specified degree (24 ^{o}C for [P$_{4,4,4,6}$][MC3S]-PNIPAM and 39 ^{o}C for [P$_{4,4,4,6}$][MC3S]-PVCL), the visual field becomes cloudy as a result of phase transition. A multitude of small particles are formed from the homogeneous solutions and they disappear again after the cooling process (Figure S5). Interestingly, the morphologies of the particles in [P$_{4,4,4,6}$][MC3S]-PNIPAM and [P$_{4,4,4,6}$][MC3S]-PVCL are different, which means that PNIPAM and PVCL have different effects on the phase transition behavior of [P$_{4,4,4,6}$][MC3S]. The particles in [P$_{4,4,4,6}$][MC3S]-PNIPAM are irregular and fragmentized, which is similar to pure [P$_{4,4,4,6}$][MC3S] solution (Figure S6). While the particles stemmed from [P$_{4,4,4,6}$][MC3S]-PVCL are regular and globular, which are called "droplets" customarily. More importantly, the appearance of the droplets is a sign of LLPS phenomenon.[37, 42] This phenomenon will be further explained in the following FT-IR analysis. In other words, the addition of PVCL makes LLPS occur in the IL-included ternary system, while PNIPAM does not. Moreover, the information of the formed IL-rich domains and water-rich matrix are shown in Figure S7 and Table S1. The results show that *ca.* 82% of solute remains in the aqueous solution in [P$_{4,4,4,6}$][MC3S]-PNIPAM, while that percentage is about 60% in [P$_{4,4,4,6}$][MC3S]-PVCL. As for IL-rich domains, *ca.* 85% of water remains in [P$_{4,4,4,6}$][MC3S]-PNIPAM system and *ca.* 47% of water remains in [P$_{4,4,4,6}$][MC3S]-PVCL one. This data is in good agreement with the following temperature-variable ^{1}H NMR analysis that a weaker dehydration process happens to IL after the addition of PNIPAM.

(a) PNIPAM/IL = 20 wt%

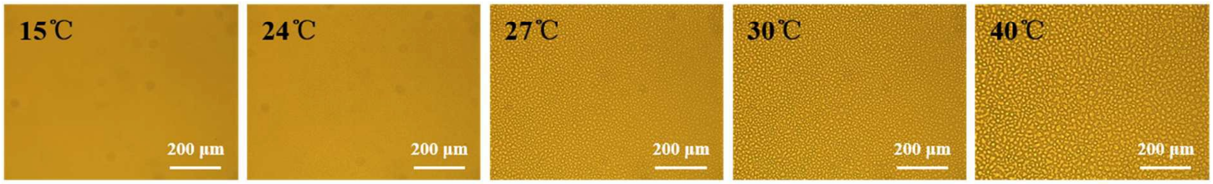

(b) PVCL/IL = 20 wt%

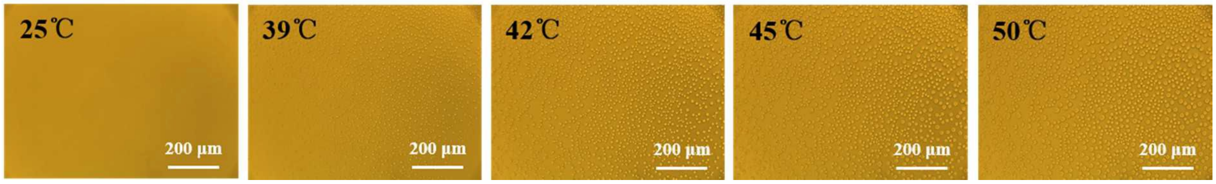

Figure 2. Optical micrographs of (a) 20% (w/v) $[P_{4,4,4,6}]$[MC3S] solution with 4% (w/v) PNIPAM and (b) 20% (w/v) $[P_{4,4,4,6}]$[MC3S] solution with 4% (w/v) PVCL (polymers/IL = 20 wt%, heating rate = 0.5 ^{o}C/min) in the heating process from 15 to 40 ^{o}C for (a) and 25 to 50 ^{o}C for (b).

Temperature-variable ^{1}H NMR

Figure 3 shows the ^{1}H NMR spectra of (a) $[P_{4,4,4,6}]$[MC3S], (b) $[P_{4,4,4,6}]$[MC3S]-PNIPAM and (c) $[P_{4,4,4,6}]$[MC3S]-PVCL in D_2O ($[P_{4,4,4,6}]$[MC3S]/D_2O = 20% (w/v), polymers/$[P_{4,4,4,6}]$[MC3S] = 20 wt%) and the assignment of various protons according to previous reports.[32, 37, 43] In the Figure 3 (b) and (c), we can distinguish the H_l, H_m of PNIPAM and H_n of PVCL from the characteristic peaks (H_a, H_b, H_c, H_d, H_f in anions, $H_{g,h}$, H_i, H_j in cations and $H_{e,k}$ in both anions and cations) of IL, which provides convenience for tracing different parts of the mixed solutions during the phase separation process.

^{1}H NMR measurement has the advantage of distinguishing the protons located in different chemical environments and tracing the change rule of them during phase transition process, which is difficult to achieve by other testing methods. Temperature-variable ^{1}H NMR spectra of $[P_{4,4,4,6}]$[MC3S] (from 25 to 50 ^{o}C), $[P_{4,4,4,6}]$[MC3S]-PNIPAM (from 15 to 40 ^{o}C) and $[P_{4,4,4,6}]$[MC3S]-PVCL (from 25 to 50 ^{o}C) solutions were presented in Figure 4 (a)-(c), respectively. Normalization was performed referencing to the integrated intensity of HDO. All the peaks shift toward lower field with a drastic decrease in intensity during the heating process, indicating the formation of aggregation in which the protons are wrapped after phase transition. To describe the phase transition degree and distinguish the differences between IL and polymers, quantitatively analyzing is necessary.

Phase separation fraction p was defined and employed to quantitatively characterize the degree of dehydration as well as phase transition. The definition of p is:

$$p = 1 - (I/I_0) \qquad (1)$$

where I is the integrated intensity of the selected resonant peak in the ^{1}H NMR spectra, and I_0 is the integrated intensity of this peak when no phase separation occurs.[37, 43-45] In this work, we took the integrated intensity obtained from the initial test temperature ($[P_{4,4,4,6}]$[MC3S]-PNIPAM for 15 ^{o}C, $[P_{4,4,4,6}]$[MC3S] and $[P_{4,4,4,6}]$[MC3S]-PVCL for 25 ^{o}C) as I_0. H_d, H_f in the anions of IL, $H_{g,h}$ in the cations of IL, H_l, H_m in PNIPAM and H_n in PVCL were chosen to analyze.

Temperature dependences of the phase separation fraction p for different protons in $[P_{4,4,4,6}]$[MC3S] are presented in Figure 4(d). After a slight decrease, p rises gradually at *ca.* 37 ^{o}C, which is in good agreement with the DSC result. The phenomenon that p undergoes a decrease process before LCST is inconspicuous (minimum of the dehydration degree p_{min} = -0.1) and it has also been found in other LCST-type ILs.[46] Additionally, we find that $[P_{4,4,4,6}]$[MC3S] experiences a relatively facile transition with a long temperature span (more than 10 ^{o}C) and the final phase separation fraction p_{max} is merely *ca.* 0.5. It reveals that $[P_{4,4,4,6}]$[MC3S] can't accomplish thorough LCST transition and $[P_{4,4,4,6}]$[MC3S] is still surrounded by many water molecules after phase transition, which is different from other thermoresponsive polymers or gels.[44] By the way, careful observation shows that the p_{max} of cations is lower than that of anions, which indicates that anions are more close to the hydrophobic cores. This phenomenon occurs not only in IL solution (Figure 4(d)) but also in IL-included ternary systems (Figure 4(e) and (f)).

Figure 4(e) shows the temperature dependences of p for D_2O solution of $[P_{4,4,4,6}]$[MC3S]-PNIPAM. Obviously, the addition of PNIPAM has changed the phase transition behavior of IL greatly and the variations of the protons in PNIPAM and IL are quite different. $[P_{4,4,4,6}]$[MC3S] has an unusual over-hydration behavior before dehydration while PNIPAM experiences a two-step transition process in $[P_{4,4,4,6}]$[MC3S]-PNIPAM solution, which has never been reported before. In a certain temperature range (15-25 ^{o}C), both IL and PNIPAM are well dissolved and the p of them are almost overlapped and close to zero. When the temperature was raised to 25 ^{o}C, the curve diverges into two. Specifically, PNIPAM begins to dehydrate, which is in good agreement with the DSC and optical microscopy results. Meanwhile, an unusual over-hydration behavior occurs to IL. This result confirms the surmise that PNIPAM dominates the phase separation of PNIPAM-involved IL solution to some extent. We believe a competitive process for water between IL and PNIPAM was captured by ^{1}H NMR. PNIPAM begins to lose complexed water at 25 ^{o}C. At the same time, IL has to form hydrogen bonds with more water, which promotes the hydration degree of IL. Between 25 to 32 ^{o}C, the p of IL continues to decrease until reaching p_{min} = -0.38, which is much lower than pure IL solution (p_{min} = -0.1). On the other hand, due to the drag effect of over-hydrated IL, the dehydration degree of PNIPAM is low. At 32 ^{o}C, both IL and PNIPAM dehydrate sharp and drastically (less than 5 ^{o}C). However, the p_{max} of IL is about 0.3, which is less than the pure IL solution (*ca.* 0.5). A weaker dehydration process happens to IL after the addition of PNIPAM.

Through the observation of Figure 4(f), we can find that the addition of PVCL has little effect on the temperature dependences of p for IL, including a higher LCST and a sharper dehydration process. The p_{min} is *ca.* 0.08 and the p_{max} is *ca.* 0.57, which are in close proximity to aforementioned pure IL solution. Only one dehydration process of [$P_{4,4,4,6}$][MC3S]-PVCL solution occurs at 39 ^{o}C, which is in accordance with the DSC and optical microscopy results. Hence, the different roles of PVCL and PNIPAM on the phase transition behavior of IL solution are obvious and tempting. However, we have to say, the final dehydration degree of PVCL and PNIPAM is much higher than that of IL, which reveals that the dehydration processes of these two thermoresponsive polymers are more complete than IL. Although temperature-variable ^{1}H NMR spectroscopy provides convenience for the study of different protons and elucidates much irreplaceable information in regard to the phase transition behavior, it is arduous for ^{1}H NMR to trace the changes of other non-proton chemical groups, such as ester group. In this case, we need to take advantage of FT-IR measurement.

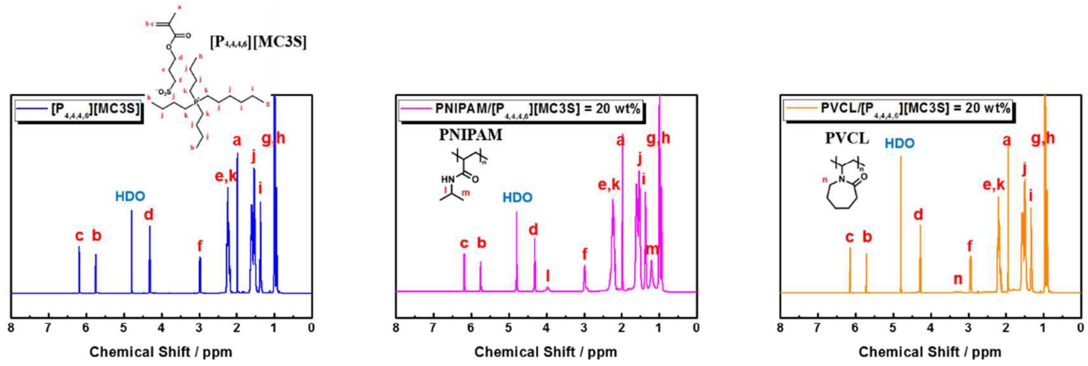

(a) (b) (c)

Figure 3. ^{1}H NMR spectra of (a) [$P_{4,4,4,6}$][MC3S], (b) [$P_{4,4,4,6}$][MC3S]-PNIPAM and (c) [$P_{4,4,4,6}$][MC3S]-PVCL in D_2O ([$P_{4,4,4,6}$][MC3S]/D_2O = 20% (w/v), polymers/[$P_{4,4,4,6}$][MC3S] = 20 wt%) and the assignments of various protons.

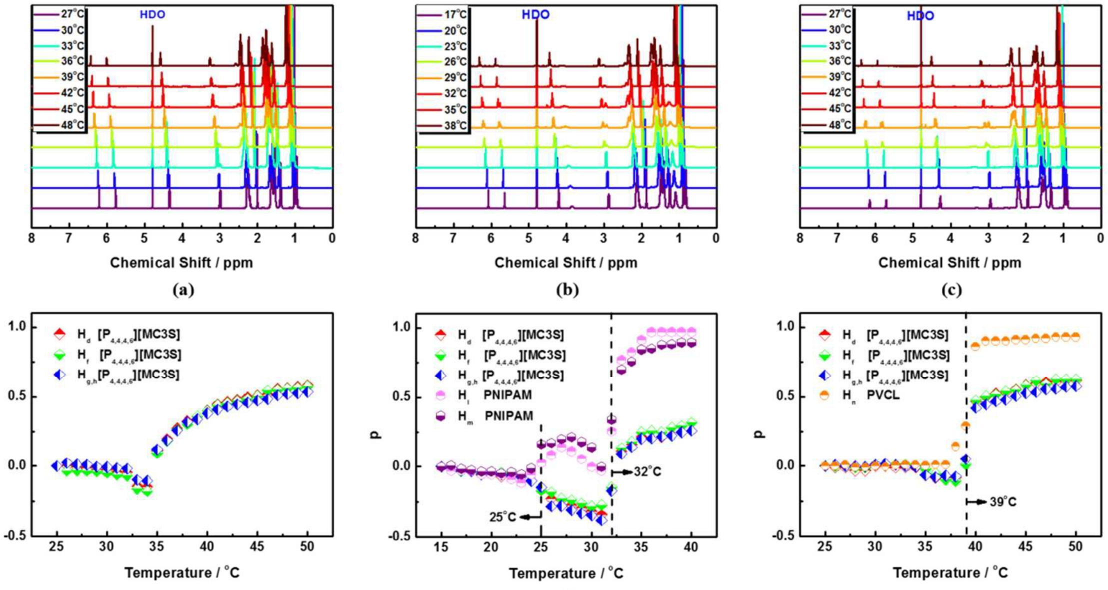

(d) (e) (f)

Figure 4. Normalized temperature-variable ^{1}H NMR spectra of (a) [$P_{4,4,4,6}$][MC3S], (b) [$P_{4,4,4,6}$][MC3S]-PNIPAM and (c) [$P_{4,4,4,6}$][MC3S]-PVCL in D_2O ([$P_{4,4,4,6}$][MC3S]/D_2O = 20% (w/v), polymers/[$P_{4,4,4,6}$][MC3S] = 20 wt%) and (bottom) their temperature dependences of phase separated fraction p for different protons, respectively.

Conventional FT-IR Analysis

Vibrational spectroscopy has been proved to be very sensitive to subtle conformational changes, especially for the thermoresponsive behavior. Here, temperature-variable FT-IR has been performed to study the changes of C=O groups during phase transition, as shown in Figure 5. It should be noted that D_2O was utilized as the solvent instead of H_2O to eliminate the overlap of the δ(O–H) band at around 1640 cm^{-1} with ν(C=O). Obviously, there exists two kind of distinguishable C=O groups in the IL-included ternary systems, one is the ester group in

$[P_{4,4,4,6}][MC3S]$ (1740-1670 cm^{-1}), the other is the amide groups in thermoresponsive polymers (1670-1580 cm^{-1} for PNIPAM and 1650-1570 cm^{-1} for PVCL). The C=O stretching bands shift to lower wavenumbers with temperature increase, which should represent dehydration process during the phase transition. Similar changes can also be found in other thermoresponsive ILs and polymers that a dehydrated condition has a lower wavenumber of C=O stretching than a hydrated one.[34-36] However, the change of ester groups is smaller than that of amide groups. Besides, the peak forms of amide groups are complicated, which reflects corresponding microscopic structures.[37] It is noted that there exists an isosbestic point in Figure 5(a) at 1638 cm^{-1}. Generally, an isosbestic point appears only when one species is quantitatively converted to another single species.[47] In the case of $[P_{4,4,4,6}][MC3S]$-PNIPAM solution, it indicates that the changes of the amide groups in PNIPAM take place between two single states without apparent intermediate conformations. As for $[P_{4,4,4,6}][MC3S]$-PVCL solution, the amide groups of PVCL have two strong bands at 1608 and 1631 cm^{-1}, which is much different from pure PVCL solution[36] and the PVCL solutions with conventional ILs[24].

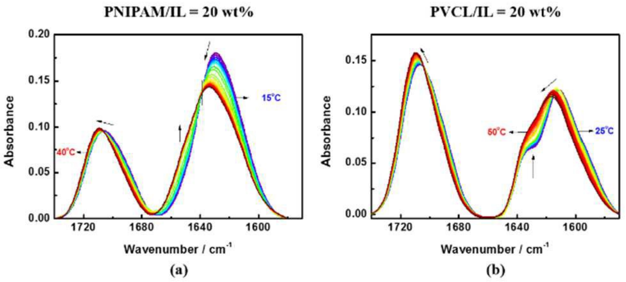

Figure 5. Temperature-dependent FT-IR spectra of (a) $[P_{4,4,4,6}][MC3S]$-PNIPAM and (b) $[P_{4,4,4,6}][MC3S]$-PVCL in D_2O ($[P_{4,4,4,6}][MC3S]/D_2O$ = 20% (w/v), polymers/$[P_{4,4,4,6}][MC3S]$ = 20 wt%) in the region of 1740-1570 cm^{-1} during heating between 15 °C to 40 °C and 25 °C to 50 °C, respectively. The temperature increment interval is 1 °C with an increasing rate of 0.5 °C/min.

The changes of peak form in amide groups are distinct and could reflect the water environment of IL indirectly. To show the changes of frequency and peak form clearly, we plotted the second derivative curves of amide C=O stretching bands, as presented in Figure 6. The minima in the second derivative curves correspond to the actual peaks in the original absorption spectra. At 15 °C (below LCST) in Figure 6(a), the pure PNIPAM and IL-PNIPAM solutions only have one strong band around 1625 cm^{-1}, which can be attributed to the vibration of C=O···D-O-D hydrogen bond in PNIPAM. When the temperature rises to 40 °C (above LCST), a new band at 1650 cm^{-1} is formed, which is assigned to the strong intra-/inter-molecular hydrogen bond C=O···D–N (PNIPAM). Compared with pure PNIPAM solution, IL-PNIPAM experiences a mild phase transition process, especially for the formation of C=O···D–N bonds. This phenomenon manifests that after phase transition, there are still plenty of water surrounding PNIPAM to hinder the formation of high-density intra-/inter-molecular hydrogen bond C=O···D–N. In other words, PNIPAM captures water more easily than IL to "break" the water structure of IL.

As for IL-PVCL in Figure 6(b), the situation is much different. Actually, there exist three peaks corresponding to three kinds of lactam groups with distinct water environments.[36, 37] The peak at 1592 cm^{-1} is fully hydrated C=O bands (lactam groups hydrogen-bonded to two water); the peak at 1608 cm^{-1} is attributed to hydrated C=O bands *v*(C=O···D-O-D) (lactam groups hydrogen-bonded to one water molecule), while the 1631 cm^{-1} one corresponds to polymer–water–polymer hydrogen bonds *v*(C=O···D-O-D···O=C) (two lactam groups hydrogen-bonded to one water). At 25 °C (below LCST), fully hydrated and hydrated C=O bands exist at the same time in pure PVCL solution. After phase transition, the intensity of fully hydrated band decreases, revealing the dehydrated process of lactam groups. While as for IL-PVCL solution, the peak at 1592 cm^{-1} disappears and the peak at 1631 cm^{-1} appears at 25 °C (below LCST), indicating that the PVCL in IL-included solution cannot fully hydrate and the relatively dehydrated polymer–water–polymer hydrogen bonds have been formed already before LCST. When the temperature reaches 50 °C (above LCST), the number of polymer–water–polymer hydrogen bonds increase with a decrease of hydrated C=O bands. Obviously, the PVCL in IL-included solution experiences a relatively thorough dehydration process in comparison to pure PVCL solution. That is to say, PVCL loses water to "make" the water structure around IL. Last but not least, the formation of polymer–water–polymer hydrogen bonds found in IL-PVCL solution is a spectroscopic sign of LLPS phenomenon.[37, 42] This provides a microscopic explanation for the different morphologies shown in the optical micrographs above.

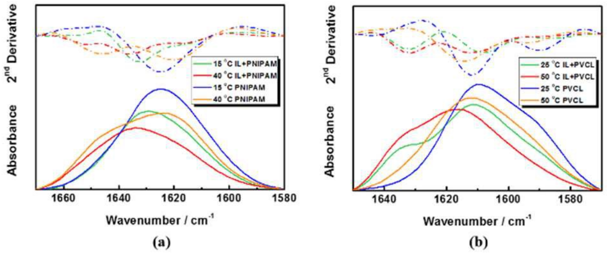

Figure 6. FT-IR and corresponding second-derivate spectra of (a) $[P_{4,4,4,6}][MC3S]$-PNIPAM-D_2O and PNIPAM-D_2O solutions, (b) $[P_{4,4,4,6}][MC3S]$-PVCL-D_2O and PVCL-D_2O solutions at different temperatures during heating.

Perturbation correlation moving window

To obtain clear phase transition points and phase transition temperature regions of distinct C=O groups in IL-included ternary systems, PCMW analysis was carried out. PCWM is a burgeoning technique, whose basic principles can be traced back to conventional moving window proposed by Thomas.[48] In 2006, the improvement of this technique was performed by Morita[49] to expand the application through introducing the perturbation variable into correlation equation. Not only does PCMW have the original ability in determining transition points as the conventional moving window did, but also it can monitor complicated spectral variations along the perturbation direction, which is difficult to detect using other conventional methods. For the convenience of discussion, tentative band assignments of $[P_{4,4,4,6}][MC3S]$-PNIPAM-D_2O and $[P_{4,4,4,6}][MC3S]$-PVCL-D_2O solutions are listed in Table 1.

Table 1. Tentative assignments of [$P_{4,4,4,6}$][MC3S]-PNIPAM-D_2O and [$P_{4,4,4,6}$][MC3S]-PVCL-D_2O solutions.

Wavenumber (cm^{-1})	Tentative Assignments
1713	*v*(Dehydrated C=O) for [$P_{4,4,4,6}$][MC3S]
1690	*v*(Hydrated C=O) for [$P_{4,4,4,6}$][MC3S]
1650	*v*(C=O···D-N) for PNIPAM
1625	*v*(C=O···D-O-D) for PNIPAM
1631	*v*(C=O···D-O-D···O=C) for PVCL
1608	*v*(C=O···D-O-D) for PVCL

Figure 7 presents PCMW synchronous and asynchronous spectra of [$P_{4,4,4,6}$][MC3S]-PNIPAM and [$P_{4,4,4,6}$][MC3S]-PVCL solutions during the phase transition process. There are two pairs of bands in the *v*(C=O) region of 1740-1570 cm^{-1}. Notably, in Figure 7 (a), the signal intensity of ester C=O (1740-1670 cm^{-1}) is weaker than that of amide C=O (1670-1580 cm^{-1}), which indicates that the amide groups in PNIPAM experience a more drastic transition process than the ester groups in IL. This conclusion is in conformity with the DSC and the temperature-variable ^{1}H NMR results that PNIPAM dominants the phase separation of PNIPAM-involved IL solution. As far as [$P_{4,4,4,6}$][MC3S]-PVCL, the almost equal intensities of ester C=O (1740-1670 cm^{-1}) and amide C=O (1650-1570 cm^{-1}) reveals the synergetic variations of IL and PVCL during the transition process.

(a) PNIPAM/IL = 20 wt%

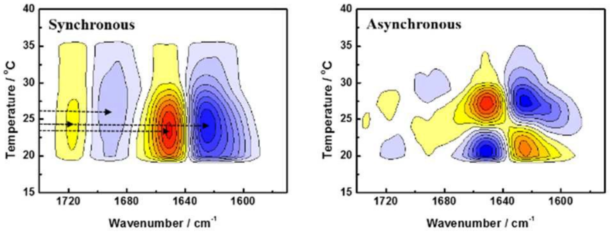

(b) PVCL/IL = 20 wt%

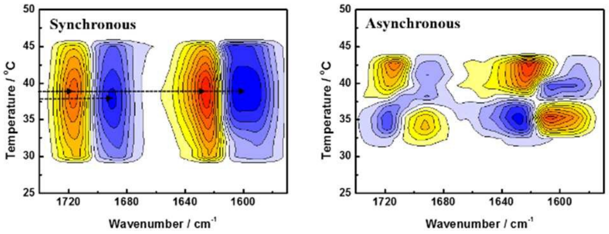

Figure 7. PCMW synchronous and asynchronous spectra of (a) PNIPAM/[$P_{4,4,4,6}$][MC3S] solution between 15 °C to 40 °C and (b) PVCL/[$P_{4,4,4,6}$][MC3S] solution between 25 °C to 50 °C during heating ([$P_{4,4,4,6}$][MC3S]/D_2O = 20% (w/v), polymers/[$P_{4,4,4,6}$][MC3S] = 20 wt%). Herein, warm colors (red and yellow) are defined as positive intensities, whereas cool colors (blue) defined as negative ones.

PCMW synchronous spectra can help us to find the transition point whereas asynchronous spectra are useful to confirm the transition temperature region by peaks with the strongest intensities. For convenience, we plotted all the points and regions read from PCMW synchronous and asynchronous spectra in Figure 8. With regard to the [$P_{4,4,4,6}$][MC3S]-PNIPAM solution (violet dotted line), the transition point of *v*(C=O···D-N) in PNIPAM is located at 23 °C, which is lower than *v*(C=O···D-O-D) in PNIPAM (24 °C), *v* (dehydrated C=O) in IL (24 °C) and *v*(hydrated C=O) in IL (26 °C), indicating that the formation of strong intra-/inter-molecular hydrogen bond C=O···D–N is the driving force for the LCST behavior. In consideration of [$P_{4,4,4,6}$][MC3S]-PVCL solution (orange dotted line), the transition point of *v*(hydrated C=O) in IL is the lowest one, which means the dehydration of ester C=O in IL dominates the phase separation behavior of [$P_{4,4,4,6}$][MC3S]-PVCL solution. Additionally, we can find that the dehydrated ester C=O responds earlier than the hydrated one in [$P_{4,4,4,6}$][MC3S]-PNIPAM, while the sequence is opposite in [$P_{4,4,4,6}$][MC3S]-PVCL solution. In other words, the ester C=O in IL would not start to dehydrate until its conformational changes were completed in [$P_{4,4,4,6}$][MC3S]-PNIPAM. Taking [$P_{4,4,4,6}$][MC3S]-PVCL into account, ester C=O is dominant for the LCST process, so it is not difficult to understand that ester C=O shows a conventional dehydration order, a hydrated ester C=O responds earlier than the dehydrated one.

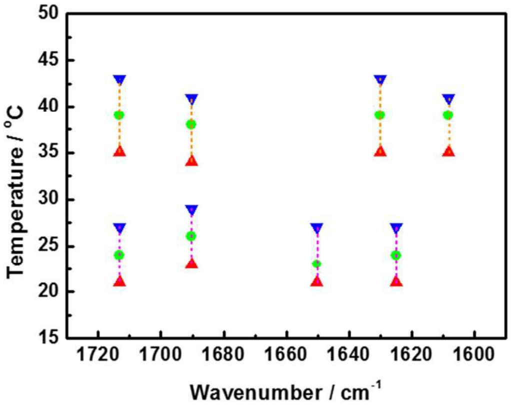

Figure 8. Corresponding transition temperatures and transition temperature regions of PNIPAM/[$P_{4,4,4,6}$][MC3S] (violet) and PVCL/[$P_{4,4,4,6}$][MC3S] (orange) solutions ([$P_{4,4,4,6}$][MC3S]/D_2O = 20% (w/v), polymers/[$P_{4,4,4,6}$][MC3S] = 20 wt%) during heating process read from PCMW synchronous and asynchronous spectra.

Proposed phase transition dynamic mechanisms of [$P_{4,4,4,6}$][MC3S]-PNIPAM and [$P_{4,4,4,6}$][MC3S]-PVCL solutions

Based on the above analysis, we can understand the impact of different thermoresponsive polymers (PNIPAM and PVCL) on the phase transition behavior of [$P_{4,4,4,6}$][MC3S] solution. The schematic illustration is shown in Figure 9.

In general, PNIPAM can "break" the water structure of [$P_{4,4,4,6}$][MC3S] to decrease the transition temperature, while PVCL can "make" the water structure to increase it. For [$P_{4,4,4,6}$][MC3S]-PNIPAM solution, there exists two phase transition steps during heating process and it is PNIPAM that dominates the phase transition. When temperature reaches 25 °C, the amide C=O in PNIPAM and the ester C=O in IL begin to dehydrate. At the same time, the C-H of IL has to form hydrogen bonds with more water to promote its hydration degree. After 32 °C, C-H groups in IL and PNIPAM dehydrate together to finish the phase transition. In the case of [$P_{4,4,4,6}$][MC3S]-PVCL solution, the relatively dehydrated polymer–water–polymer hydrogen bond C=O···D-O-D···O=C has been formed already before LCST due to the competition for water. Moreover, the phase separation behavior of [$P_{4,4,4,6}$][MC3S]-PVCL occurs at 39

°C, which is dominated by [$P_{4,4,4,6}$][MC3S] with a LLPS phenomenon.

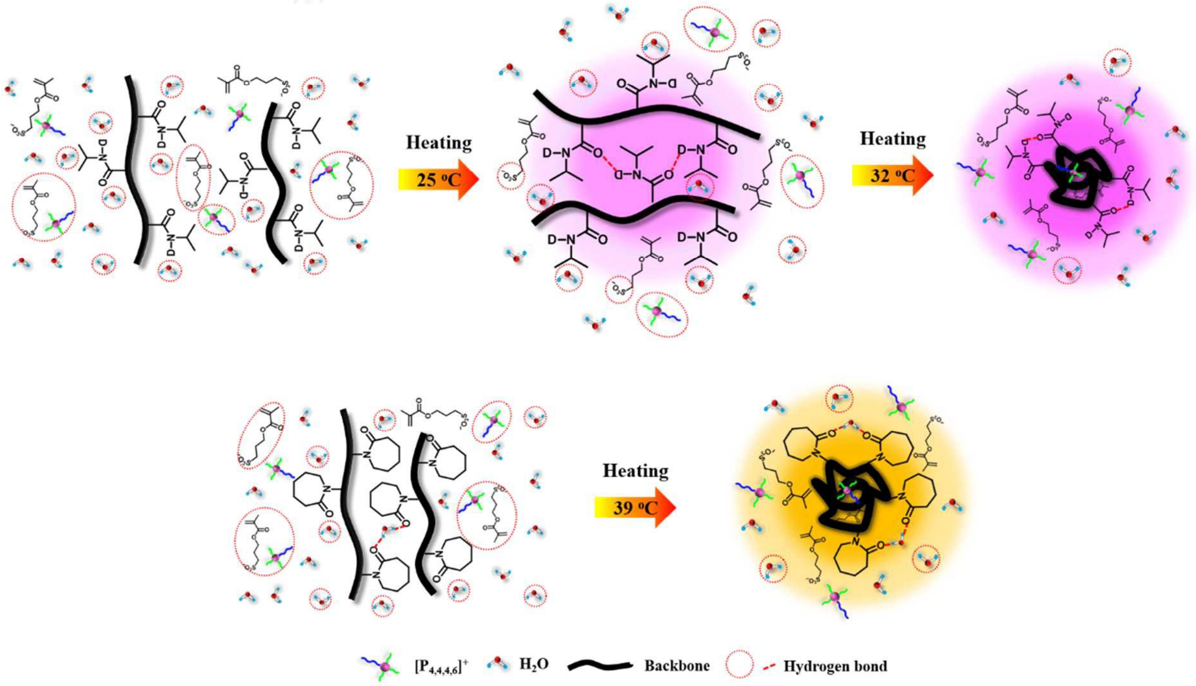

Figure 9. Schematic illustration of the dynamic changing process of [$P_{4,4,4,6}$][MC3S]-PNIPAM (top) and [$P_{4,4,4,6}$][MC3S]-PVCL (bottom) solutions during heating.

Conclusions

In this paper, DSC, optical microscopy, temperature-variable ^{1}H NMR and FT-IR in combination with the PCMW technique are utilized to explore the influence of different thermoresponsive polymers (PNIPAM and PVCL) on the phase transition behavior of thermoresponsive ionic liquid ([$P_{4,4,4,6}$][MC3S]) solution.

It is interesting that PNIPAM can drastically decrease the LCST of [$P_{4,4,4,6}$][MC3S] to 25 °C, while PVCL can slightly increase it to 39 °C. This is attributed to the effect that PNIPAM can “break” the water structure to decrease the LCST of [$P_{4,4,4,6}$][MC3S], while PVCL can “make” the water structure to increase it. What’s more, the morphologies of the phase transition in [$P_{4,4,4,6}$][MC3S]-PNIPAM and [$P_{4,4,4,6}$][MC3S]-PVCL solutions are different. LLPS phenomenon occurs in [$P_{4,4,4,6}$][MC3S]-PVCL solution, while it doesn’t happen in [$P_{4,4,4,6}$][MC3S]-PNIPAM one. According to temperature-variable ^{1}H NMR, we successfully traced a two-step transition behavior in [$P_{4,4,4,6}$][MC3S]-PNIPAM solution: one is for PNIPAM units (*ca.* 25°C), the other is for the corporate dehydration of [$P_{4,4,4,6}$][MC3S] and PNIPAM (*ca.* 32°C). In the first step, [$P_{4,4,4,6}$][MC3S] experiences an unusual over-hydration process due to the competition for water between IL and PNIPAM. For [$P_{4,4,4,6}$][MC3S]-PVCL, there is only one transition process at *ca.* 39 °C. FT-IR spectra demonstrated the changes of ester and amide C=O groups during phase transition. Unexpectedly, the relatively dehydrated polymer–water–polymer hydrogen bond C=O···D-O-D···O=C has been formed already before LCST in [$P_{4,4,4,6}$][MC3S]-PVCL. Finally, PCMW was employed to illuminate the phase transition dynamic mechanisms of [$P_{4,4,4,6}$][MC3S]-PNIPAM and [$P_{4,4,4,6}$][MC3S]-PVCL solutions. The formation of strong intra-/inter-molecular hydrogen bond C=O···D–N in PNIPAM is the driving force for the LCST phenomenon of [$P_{4,4,4,6}$][MC3S]-PNIPAM solution, while it is the [$P_{4,4,4,6}$][MC3S] that dominates the phase separation of [$P_{4,4,4,6}$][MC3S]-PVCL solution. Additionally, the formation of polymer–water–polymer hydrogen bonds C=O···D-O-D···O=C is a microscopic explanation for macroscopic LLPS phenomenon. Thus, the phase transition dynamic mechanisms of [$P_{4,4,4,6}$][MC3S]-PNIPAM and [$P_{4,4,4,6}$][MC3S]-PVCL are clarified, which could be helpful to understand the versatile and complex interactions between ILs and polymers.

Acknowledgements

We gratefully acknowledge the financial support from the National Science Foundation of China (NSFC) (Nos. 21274030, 51473038).

Notes and references

† Electronic Supplementary Information (ESI) available.

1 N. V. Plechkova and K. R. Seddon, *Chem. Soc. Rev.*, 2008, **37**, 123-150.
2 J. Lu, F. Yan and J. Texter, *Prog. Polym. Sci.*, 2009, **34**, 431-448.
3 R. D. Rogers and K. R. Seddon, *Science*, 2003, **302**, 792-793.
4 C. Chiappe and D. Pieraccini, *J. Phys. Org. Chem.*, 2005, **18**, 275-297.
5 N. Isambert, M. d. M. S. Duque, J.-C. Plaquevent, Y. Genisson, J. Rodriguez and T. Constantieux, *Chem. Soc. Rev.*, 2011, **40**, 1347-1357.
6 J. P. Hallett and T. Welton, *Chem. Rev.*, 2011, **111**, 3508-3576.
7 R. Sheldon, *Chem. Commun.*, 2001, 2399-2407.
8 Q. Zhang, S. Zhang and Y. Deng, *Green Chem.*, 2011, **13**, 2619-2637.
9 M. Armand, F. Endres, D. R. MacFarlane, H. Ohno and B. Scrosati, *Nat. Mater.*, 2009, **8**, 621-629.

10 H. Liu, Y. Liu and J. Li, *Phys. Chem. Chem. Phys.*, 2010, **12**, 1685-1697.

11 J. F. Liu, J. A. Jonsson and G. B. Jiang, *Trac-Trends Anal. Chem.*, 2005, **24**, 20-27.

12 P. Sun and D. W. Armstrong, *Anal. Chim. Acta*, 2010, **661**, 1-16.

13 X. Han and D. W. Armstrong, *Accounts Chem. Res.*, 2007, **40**, 1079-1086.

14 A. Berthod, M. Ruiz-Angel and S. Carda-Broch, *J. Chromatogr. A*, 2008, **1184**, 6-18.

15 P. Kubisa, *Prog. Polym. Sci.*, 2004, **29**, 3-12.

16 D. Mecerreyes, *Prog. Polym. Sci.*, 2011, **36**, 1629-1648.

17 J. Yuan, D. Mecerreyes and M. Antonietti, *Prog. Polym. Sci.*, 2013, **38**, 1009-1036.

18 Y. Kohno, S. Saita, Y. Men, J. Yuan and H. Ohno, *Polym. Chem.*, 2015, **6**, 2163-2178.

19 J. L. Anderson, J. Ding, T. Welton and D. W. Armstrong, *J. Am. Chem. Soc.*, 2002, **124**, 14247-14254.

20 A. Pinkert, K. N. Marsh, S. Pang and M. P. Staiger, *Chem. Rev.*, 2009, **109**, 6712-6728.

21 D. Constantinescu, H. Weingaertner and C. Herrmann, *Angew. Chem.-Int. Edit.*, 2007, **46**, 8887-8889.

22 P. M. Reddy and P. Venkatesu, *J. Phys. Chem. B*, 2011, **115**, 4752-4757.

23 Z. Wang and P. Wu, *RSC Adv.*, 2012, **2**, 7099-7108.

24 W. Li and P. Wu, *Polym. Chem.*, 2014, **5**, 761-770.

25 Y. Kohno, S. Saita, K. Murata, N. Nakamura and H. Ohno, *Polym. Chem.*, 2011, **2**, 862-867.

26 Y. Xiong, J. Liu, Y. Wang, H. Wang and R. Wang, *Angew. Chem.-Int. Edit.*, 2012, **51**, 9114-9118.

27 Y. Kohno and H. Ohno, *Chem. Commun.*, 2012, **48**, 7119-7130.

28 K. Fukumoto and H. Ohno, *Angew. Chem.-Int. Edit.*, 2007, **46**, 1852-1855.

29 Y. Kohno, H. Arai, S. Saita and H. Ohno, *Aust. J. Chem.*, 2011, **64**, 1560-1567.

30 Y. Kohno and H. Ohno, *Phys. Chem. Chem. Phys*, 2012, **14**, 5063-5070.

31 Y. Kohno and H. Ohno, *Aust. J. Chem.*, 2012, **65**, 91-94.

32 Y. Kohno, Y. Deguchi and H. Ohno, *Chem. Commun.*, 2012, **48**, 11883-11885.

33 Y. Men, H. Schlaad and J. Yuan, *ACS Macro Lett.*, 2013, **2**, 456-459.

34 G. Wang and P. Wu, *Soft Matter*, 2015, **11**, 5253-5264.

35 B. Sun, Y. Lin, P. Wu and H. W. Siesler, *Macromolecules*, 2008, **41**, 1512-1520.

36 S. Sun and P. Wu, *J. Phys. Chem. B*, 2011, **115**, 11609-11618.

37 J. Spevacek, J. Dybal, L. Starovoytova, A. Zhigunov and Z. Sedlakova, *Soft Matter*, 2012, **8**, 6110-6119.

38 S. Sun and P. Wu, *Macromolecules*, 2013, **46**, 236-246.

39 Y. W. Ding, X. D. Ye and G. Z. Zhang, *Macromolecules*, 2005, **38**, 904-908.

40 Y. J. Zhang, S. Furyk, D. E. Bergbreiter and P. S. Cremer, *J. Am. Chem. Soc.*, 2005, **127**, 14505-14510.

41 W. Li and P. Wu, *Soft Matter*, 2014, **10**, 6161-6171.

42 T. Li, H. Tang and P. Wu, *Soft Matter*, 2015, **11**, 3046-3055.

43 L. Starovoytova, J. Spevacek and M. Ilavsky, *Polymer*, 2005, **46**, 677-683.

44 J. Spevacek, *Curr. Opin. Colloid Interface Sci.*, 2009, **14**, 184-191.

45 H. Tang, B. Zhang and P. Wu, *Soft Matter*, 2014, **10**, 7278-7284.

46 W. Li and P. Wu, *Polym. Chem.*, 2014, **5**, 5578-5590.

47 B. S. Berlett, R. L. Levine and E. R. Stadtman, *Anal. Biochem.*, 2000, **287**, 329-333.

48 M. Thomas and H. H. Richardson, *Vib. Spectrosc.*, 2000, **24**, 137-146.

49 S. Morita, H. Shinzawa, I. Noda and Y. Ozaki, *Appl. Spectrosc.*, 2006, **60**, 398-406.

For Table of Contents Entry

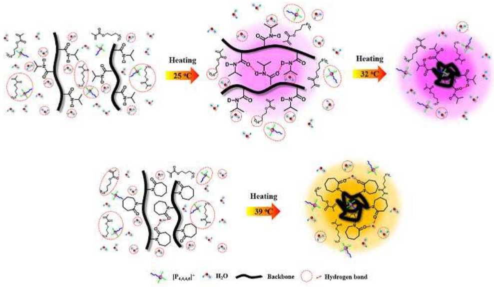

Schematic illustration of the dynamic changing process of [P$_{4,4,4,6}$][MC3S]-PNIPAM (top) and [P$_{4,4,4,6}$][MC3S]-PVCL (bottom) solutions during heating.